Frequency Stabilization of Power-Combining Grid Oscillator Arrays

Wenzhang Wang, *Member, IEEE*, and L. Wilson Pearson, *Fellow, IEEE*

***Abstract*—In this paper, we report results of phase locking of grid oscillator arrays. First, a voltage-controlled grid oscillator array with a center frequency of 4.7 GHz and with a 300-MHz electric tuning range was locked to a frequency synthesizer through a phase-locked loop. Second, a 4×4 and a 6×6 grid oscillator arrays were locked by way of the injection locking. In both methods, a simple loop antenna mounted on the reflection mirror was used for taking/injecting signal from/to the array. Results show that the phase noise performance is improved significantly in the locked oscillator arrays.**

***Index Terms*—Frequency stabilization, grid oscillator, injection locking, phase-locked loop, spatial power combining, VCO.**

I. Introduction

SPATIAL power-combining techniques have attracted much attention in the past decades for their capability of combining power efficiently from a large number of active devices at millimeter-wave frequencies [1]–[16]. Although many different spatial combining schemes have been reported, they can generally be classified, according to their functions, as amplifier combining arrays and oscillator combining arrays. In the case of an oscillator array power combiner, all individual devices or oscillators in the array must be synchronized so that the power that they radiate combines coherently in the radiation field.

Many applications require that the microwave sources not only provide high power, but also have high-frequency stability and low phase-noise performances. Indeed, coupled oscillator systems cohere to a single frequency better when the individual oscillators are low in Q factor. Even though the phase noise improves with the increasing number of active devices from where the power is combined, an oscillator array power combiner without any external frequency stabilization circuitry is likely not to meet the phase-noise and frequency-stability requirements for a system in which the oscillator is to be used. We have observed in our experiment that objects placed in front of an oscillator array affect the oscillation frequency. This contributes mainly to the direct coupling between the resonant circuits in the array and free space. It is also possible that the array be injection locked or synchronized to an interference source and fail to function when it is illuminated by an interference source with frequency close to the array frequency.

Efforts have been made in the past to synchronize and stabilize the oscillation frequency of an oscillator power-combining array. Dinger *et al.* [9] reported a three-element oscillator array using patch antennas and IMPATT diodes. In this array, the center element is injection locked to a reference signal and the array is synchronized by mutual coupling between the elements. Recently, York's group [10] has done a systematic study of injection locking and phase noise of coupled oscillator arrays.

In this paper, both loop-phase-locking and injection-locking techniques are explored for the frequency stabilization of power-combining grid oscillator arrays. Experimental results for loop-phase-locked 4×4 grid oscillator arrays and for injection-locked 4×4 and 6×6 grid oscillator arrays are presented in Sections III and IV, respectively. It has been shown that both loop phase locking and injection locking of grid oscillator arrays can improve the phase-noise performance. The design and performance of a voltage-controlled 4×4 grid oscillator array are also presented. A 300-MHz frequency tuning range at 4.7 GHz was achieved with the maximum calculated effective isotropic radiated power of 29 dBm.

II. Voltage-Controlled Grid Oscillator Arrays

Voltage-controlled grid oscillators (VCGOs) have been realized in three ways: namely, a two-plane structure in which the transistors and varactors are on different substrates or on the opposite sides of one substrate [11], a single-plane gate-feedback structure [12], [13], and single-plane source-feedback structure [14]. In the work reported here, we used the third structure due to its potential of wider tuning range or, equivalently, high tuning-voltage sensitivity.

Fig. 1 shows the physical layout of the 16-element (in a 4×4 configuration) single-plane source-feedback VCGO array. The transistors are placed at the cross of vertical and horizontal conductive strips. The gate and drain terminals of the transistors are connected to the vertical strips, while the source terminals are connected to the horizontal strips. Varactor diodes are integrated to the array by breaking the vertical gate conducting strips and placing varactor diodes across these gaps. Bias voltages are applied to the devices via horizontal conducting strips (the narrow horizontal lines in Fig. 1).

It has been pointed out in [15] that the edge elements play an important role in the stable operation of a grid oscillator array. If the edge elements are not designed properly, the grid oscillator array may oscillate at multiple frequencies. To overcome this problem, *adjustable length* open stubs are added to the upper and lower edge elements, as shown in Fig. 1.

Manuscript received December 7, 1999. This work was supported by the Federal Aviation Administration's "Millimeter Wave Integrated Circuit Antenna Imaging Array" under Contract 93-G-047, and by the Army Research Office Multidisciplinary University Research Initiative "Quasi-Optical Power Combining" Project under Grant DAAG 55-97-0132.

W. Wang was with the Department of Electrical and Computer Engineering, Clemson University, Clemson, SC 29634-0915 USA. He is now with the Telaxis Communications Corporation, South Deerfield, MA 01373 USA.

L. W. Pearson is with the Department of Electrical and Computer Engineering, Clemson University, Clemson, SC 29634-0915 USA.

Publisher Item Identifier S 0018-9480(02)04052-8.

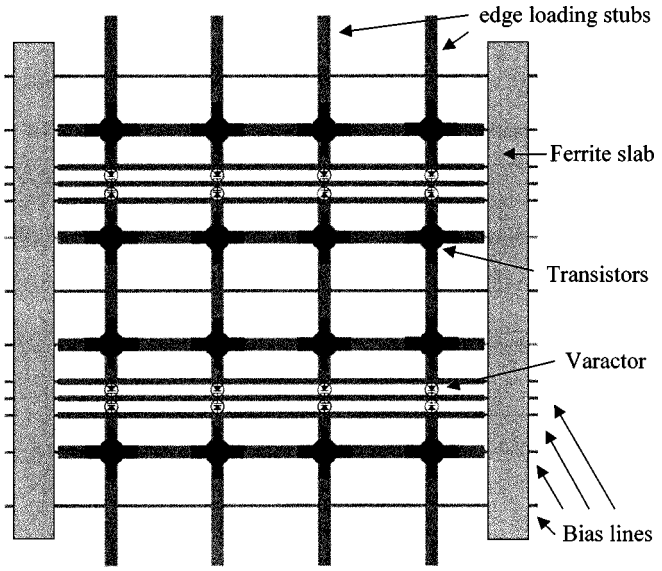

Fig. 1. Circuit layout of VCGO.

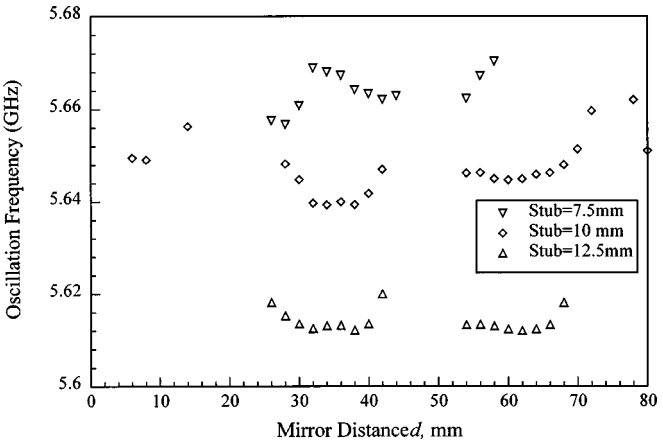

Fig. 2. Oscillation frequency versus mirror distance for the grid array without varactor diodes.

Two 4×4 grid arrays with the grid patterns shown in Fig. 1 were fabricated on 0.01-in (0.254-mm)-thick RT/Duroid 5880 substrate. The unit cell size was designed to be 8×8 mm^2. The vertical (gate and drain) conducting strips and the horizontal source conducting strips have the same width of 1 mm. The width of drain and gate bias lines was 0.2 mm, the width of varactor bias lines was 0.5 mm, and the gap for the varactors was 0.5 mm. Both arrays used the same type of transistors (FHX35LG). In order to evaluate the effects of the weakened coupling between rows, varactors (MSV-34, 069-C11) were attached to one array only. When the varactor is biased at -4 V, the junction capacitance is approximately 1 pF. To improve the mechanical stability of the array, a 0.03-in-thick RT/Duroid 5870 substrate was attached to the back of the arrays.

The measurements of these two oscillator arrays were performed in an anechoic chamber. The description of the measurement setup for grid oscillator arrays can be found in [15]. The grid array without varactor diodes was measured first and the measured oscillation frequency was plotted in Fig. 2 as functions of mirror distance for three different edge stub lengths when the array was biased at $V_{\rm ds} = 5$ V and $I_{\rm ds} = 165$ mA. It was found that the mutual locking in the array breaks down when the mirror distance was less than 26 mm or between 42–54 mm. The locking failure expresses itself through oscillations at several frequencies simultaneously.

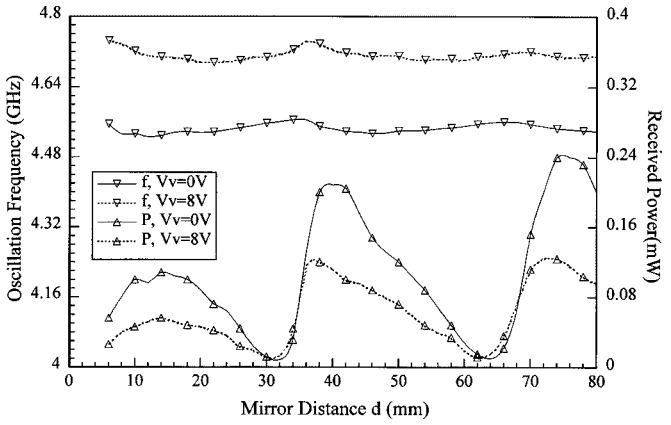

Fig. 3. Oscillation frequency versus mirror distance for the grid array with varactors.

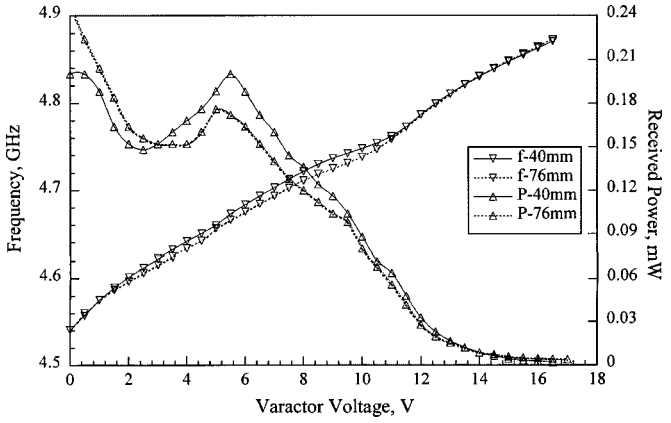

Fig. 4. Measured electrical tuning properties of the VCGO array.

For the grid array with varactor diodes, the measured results showed great improvement in the spectral purity. The tighter coupling between the neighboring rows of active devices through varactors helped the mutual locking of oscillation frequency in the array. This, however, does not mean that the multifrequency oscillation can be eliminated merely by shorting the varactors or by increasing the capacitance of the varactor used. When the stub length was 12.5 mm, we did not observe any mode jumping or multifrequency oscillation phenomena. Fig. 3 shows the oscillation frequency of the grid array with varactor diodes versus the mirror distance when the edge stub length was 12.5 mm and transistors were biased at $V_{\rm ds} = 5$ V and $I_{\rm ds} = 165$ mA. The frequency varied about 40 MHz when the mirror distance changed. The power received by the horn antenna is also plotted in the figure. The maximum isotropic radiated power [16] was calculated to be 29 dBm at the mirror distance of 76 mm. Minimum power occurred when the mirror distance was 32 and 64 mm, which were approximately a half-wavelength and one wavelength, respectively.

Fig. 4 gives the measured oscillation frequency as functions of the voltage applied to the varactor diodes when the reflection mirror was placed at 40 and 76 mm behind the grid. The overall

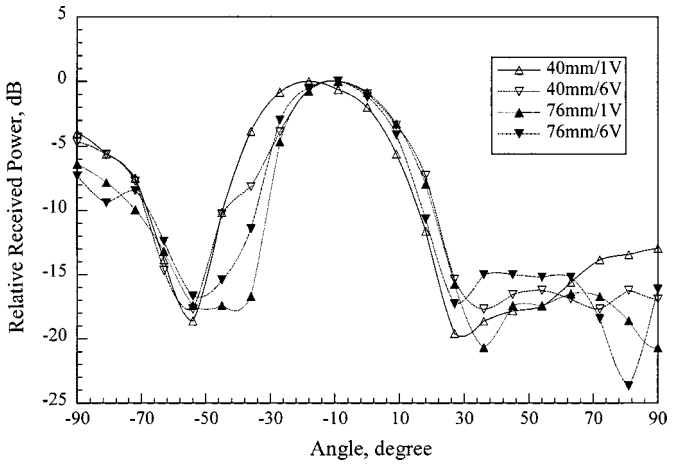

Fig. 5. Measured H-plane radiation pattern of the VCGO array.

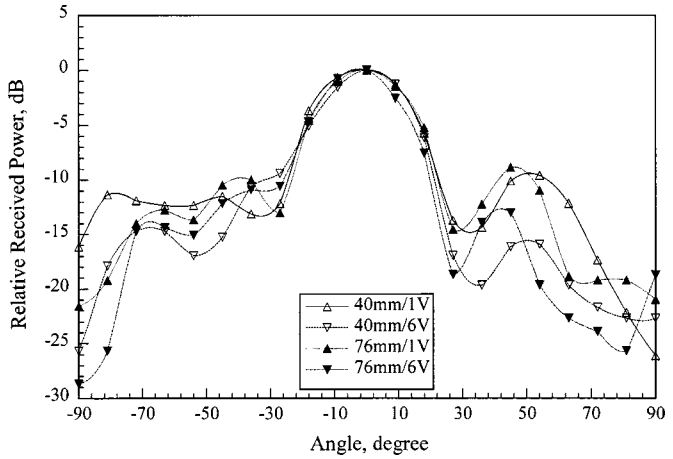

Fig. 6. Measured E-plane radiation pattern of the VCGO array.

frequency tuning range is about 330 MHz when the varactor bias voltage changes from 0 to 17 V, and the frequency-tuning slope is approximately 20 MHz/V. It can also be seen that the received power varies from above 0.15 mW to below 0.03 mW, and the tuning range with power variation less than 3 dB is about 150 MHz.

The radiation patterns of the VCGO with edge stub length of 12.5 mm were measured for the mirror distances of 40 and 76 mm and the varactor bias voltage of 1 and 6 V. The H- and E-plane patterns are shown in Figs. 5 and 6, respectively. The asymmetric H-plane patterns suggest that a progressive phase shift is present across the array, as pictured in Fig. 1. The effects of varactor tuning on the radiation beam width are small compared to the effects of the mirror distance, which is also weakened when the array becomes large.

III. Loop-Phase-Locked Grid Oscillator Array

A basic phase-locked loop consists of a voltage-controlled oscillator (VCO), phase detector, and loop filter [17]. Fig. 7 illustrates the block diagram of a phase-locked loop. The phase detector compares the phase of the reference signal against the phase of the VCO and converts the phase difference between the two inputs into a voltage signal. This voltage signal is then filtered by the loop filter and applied to the VCO. When the loop is

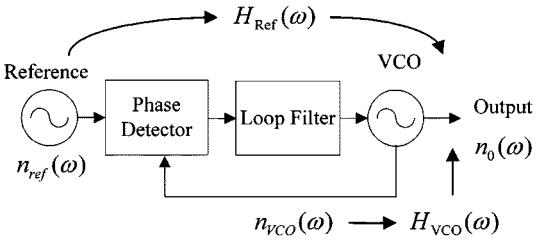

Fig. 7. Block diagram of a phase-locked loop.

in the locked state, the oscillation frequency of the VCO tracks exactly the frequency of the reference signal.

When a perfect integrator circuit is used as a loop filter, the phase-locked loop becomes a second-order loop. The closed-loop phase transfer function $H_{\text{Ref}}(\omega)$, which is the phase transfer function from reference signal to the output of the phase-locked loop, and $H_{\text{VCO}}(\omega)$, the phase transfer function from the free-running VCO to the loop output, can be written as

$$H_{\text{Ref}}(\omega) = \frac{j2\xi\omega_n\omega + \omega_n^2}{-\omega^2 + j2\xi\omega_n\omega + \omega_n^2} \tag{1}$$

$$H_{\text{VCO}}(\omega) = \frac{-\omega^2}{-\omega^2 + j2\xi\omega_n\omega + \omega_n^2} \tag{2}$$

where $\omega = 2\pi\Delta f$, Δf represents the frequency-off-carrier; ω_n and ξ are the natural resonant frequency and the damping factor of the loop, respectively, which can be represented as

$$\omega_n^2 = \frac{K_0 K_d}{\tau_1} \tag{3}$$

$$\xi = \frac{\tau_2\omega_n}{2}. \tag{4}$$

In the above equations, K_d and K_0 are the phase sensitivity of the phase detector and the tuning slope of the VCO, respectively. τ_1 and τ_2 are the time constants of the perfect integrator. Let the phase noise of the reference signal be $n_{\text{ref}}(\omega)$ and that of the free-running VCO be $n_{\text{VCO}}(\omega)$. The total phase noise of the locked oscillator can then be represented as

$$n_0(\omega) = n_{\text{VCO}}(\omega)|H_{\text{VCO}}(\omega)|^2 + n_{\text{ref}}(\omega)|H_{\text{Re}\,f}(\omega)|^2. \tag{5}$$

It can be seen that the phase noise of the locked signal is dominated by the reference signal within the loop bandwidth and by the VCO outside the loop bandwidth. An optimum design of the phase-locked loop that gives the best phase-noise performance can be achieved by choosing the loop bandwidth equal to the frequency at which the VCO and the reference signal have the same phase noise.

In order to phase lock the grid oscillator, a sample signal from the VCGO is needed for the phase detector to detect phase errors between the VCGO and reference signal. One way to take sample signal is to place a receiving antenna in front of the array so that part of the radiated power from the array can be collected. The disadvantage associated with this method is that the receiving antenna in front of the array blocks radiation. The second disadvantage is that the scattered field due to objects in front of the array may get into the antenna and affect the phase

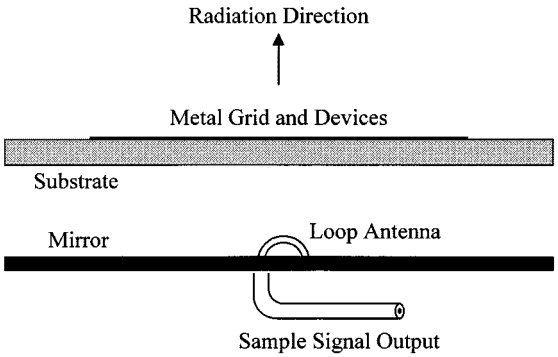

Fig. 8. Sample signal is taken from a small loop antenna mounted on the reflect mirror.

of the sampling signal, which may modulate the VCGO through the phase-locked loop. In our experiment, the VCGO described in the previous section was modified to a dual-output configuration. Fig. 8 depicts the structure of the modified VCGO array for the phase-locked-loop application. A small loop antenna was mounted on the mirror surface that backs the active grid array and sample signal was coupled out through the loop antenna. The loop antenna is made so small that its presence poses little effect on the oscillator performance. When the diameter of the loop is 7 mm, the power collected by it was measured to be around 0.07 mW for the 4×4 VCGO. This is negligibly small when compared to the power that the grid oscillator can produce, but is big enough to feed the phase detector. We observed that the oscillation frequency changed only a few megahertz after the loop was installed. This structure has also been used, in the following section, for coupling power into the grid oscillator array for injection locking of a grid oscillator array. We point out that other structures such as slot antennas and coupling apertures are more suitable for taking samples in the millimeter-wave range.

The phase detector used in this study was a commercially available balanced diode mixer ZMX-10G made by Mini-Circuits Inc., Brooklyn, NY. It is designed to operate up to 10 GHz with an IF frequency from dc to 2 GHz. When used for phase detection, it has sinusoidal phase–voltage relationship. The phase detection sensitivity was measured with two HP microwave frequency synthesizers. Both synthesizers are phase locked to the same reference crystal oscillator so that the two input signals of the phase detector are coherent. The frequencies of the two signals are intentionally set to have a 1-kHz offset so that the phase–voltage relationship can be measured with an oscilloscope. The measured phase sensitivity of the phase detector is plotted in Fig. 9 as a function of the RF input power with the local oscillator (LO) power set to $+5$ dBm.

The loop filter, as sketched in Fig. 10, consists of three operational amplifiers or three stages. The first stage serves as an input isolation stage and has a voltage gain of ten. The second stage is a perfect integrator, whose time constants $\tau_1 = R_aC$ and $\tau_2 = R_bC$ determine the bandwidth of the loop. The last stage is a level shift circuit that matches the output voltage range of the perfect integrator circuit ($-14 \sim +14$ V) to the input voltage range ($0 \sim +14$ V) of the VCGO.

The phase noise of the free-running grid oscillator was too large to be measured by the method described. In order to demonstrate phase locking, we took the loop bandwidth

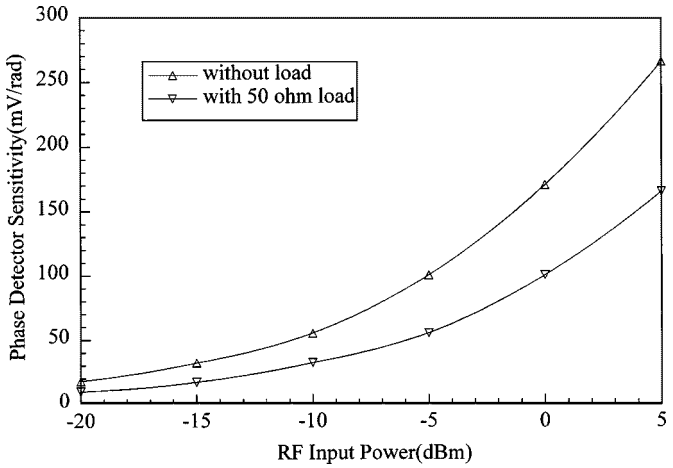

Fig. 9. Sensitivity of the phase detector when LO power is 5 dBm.

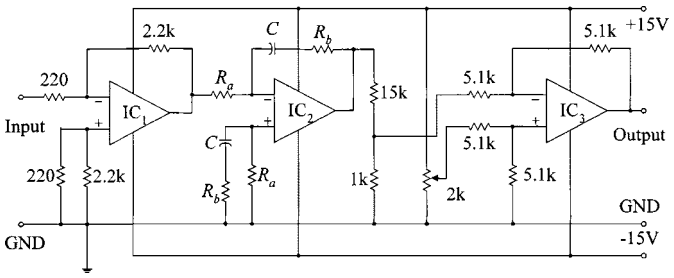

Fig. 10. Circuit configuration of the loop filter.

to be 100 kHz and the damping factor $\xi = 1$. From (1), the 3-dB noise bandwidth of the phase-locked loop with a perfect integrator can be expressed as

$$B_{3\,\mathrm{dB}} = \frac{\omega_n}{2\pi}\left[2\xi^2 + 1 + \sqrt{(2\xi^2+1)^2+1}\right]^{1/2}. \quad (6)$$

The natural resonant frequency can then be calculated as

$$\omega_n = 2\pi B_{3\,\mathrm{dB}}\left[2\xi^2 + 1 + \sqrt{(2\xi^2+1)^2+1}\right]^{-1/2} = 253.3\ \mathrm{krad/S}.$$

In the design of the loop filter, both the frequency tuning slope of the VCGO and the phase sensitivity of the phase detector need to be modified to the effective values immediately at the output and the input of the filter stage. The modified values are $K_0 = 1.33$ MHz/V and $K_d = 0.17$ V/rad. One can obtain the time constants as

$$\tau_1 = \frac{K_0K_d}{\omega_n^2} = 2.2219 \times 10^{-5}\ \mathrm{S}$$

$$\tau_2 = \frac{2\xi}{\omega_n} = 7.896 \times 10^{-6}\ \mathrm{S}. \quad (7)$$

The filter resistors can then be obtained by choosing $C = 0.022\ \mu F$ to be $R_a = \tau_1/C = 1$ kΩ and $R_b = \tau_2/C = 360\ \Omega$.

Using the component values calculated above and by adjusting the potentiometer W in Fig. 10, the VCGO was phase locked to a microwave frequency synthesizer. The spectra of both the free-running grid oscillator array and the phase-locked grid array were measured using an HP8592 spectrum analyzer.

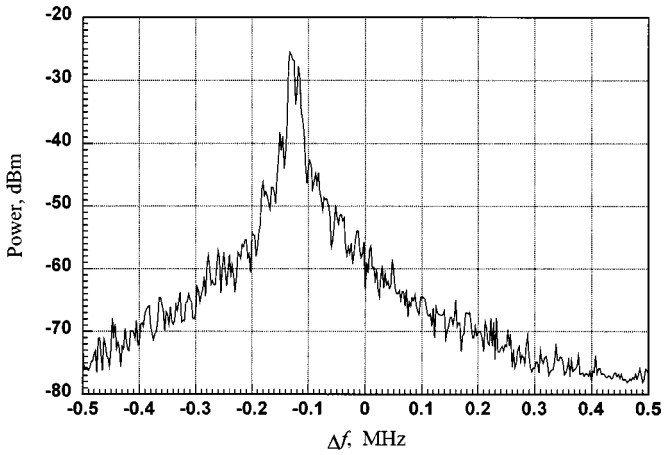

(a)

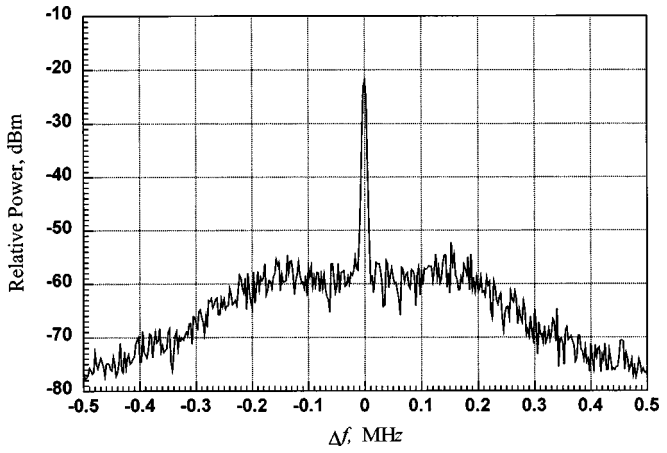

(b)

Fig. 11. Spectra of: (a) free-running and (b) loop-phase-locked grid oscillator; center frequency 4.643 GHz, spectrum analyzer filter bandwidth 3 kHz.

The results are given in Fig. 11. From these figures, one can see that the phase-noise improvement due to the phase locking is significant. A rough measurement of the phase noise has been done with an HP8575/141T spectrum analyzer [18] by setting the bandwidth of the input filter of the spectrum analyzer much smaller than the frequency-off-carrier (Δf). The phase noise is then estimated to be the difference between the power readings (in decibels) from the spectrum analyzer at the frequency-off-carrier and at the carrier frequency, which is divided by the filter bandwidth. The limit of this method is that it requires the signal to be measured has a high-frequency stability. Therefore, only the phase-locked grid array was measured and the results are listed in Table I together with the phase noise of the reference source. Note that the synthesizer phase noise data are taken from the specifications in the manual. It is clear from the measured spectra in Fig. 11 and the phase noise data in Table I that the loop was not designed to work at optimum phase-noise bandwidth. The phase-noise performance of the locked grid oscillator array can be improved by increasing the noise bandwidth of the phase-locked loop.

IV. Injection Locking of Grid Oscillators

The other way to lock a grid oscillator is to use the injection-locking technique. When an oscillator is injected by a signal with its frequency very close to that of the oscillator, the oscillator will be locked or synchronized to the injected signal [19]. The frequency stability and phase noise of the locked oscillator will be improved up to the same as that of the injected signal. This technique has been successfully used for frequency stabilization of microwave and millimeter-wave oscillators. The injected signal usually has higher frequency stability and lower phase noise, but at a lower power level. The oscillator to be locked, however, has poor frequency stability, but is capable of providing high output power. Let the injected power be P_i and the oscillation power be P_o. Under the locked condition, the locking range is then [19]

$$\Delta\omega_m = \frac{\omega_0}{Q_{\text{ext}}}\sqrt{\frac{P_i}{P_0}} \tag{8}$$

where w_0 is the free-running oscillation frequency and Q_{ext} is the external quality factor of the resonant circuits in the oscillator to be injection locked.

In an injection-locked oscillator, the phase noise transferred from the reference source and the free-running oscillator to the output of the locked oscillator are characterized by the noise power suppression factors S_1 and S_2. These factors are defined as [19], [20]

$$S_1(\omega) = \frac{1}{1+\left(\dfrac{\omega}{\Delta\omega_m}\right)^2} \tag{9}$$

for noise due to the reference signal and

$$S_1(\omega) = \frac{\left(\dfrac{\omega}{\Delta\omega_m}\right)^2}{1+\left(\dfrac{\omega}{\Delta\omega_m}\right)^2} \tag{10}$$

for noise due to the oscillator. The total noise output is the sum of the two, i.e.,

$$n_0(\omega) = S_1(\omega)n_{\text{ref}}(\omega) + S_2(\omega)n_{\text{osc}}(\omega). \tag{11}$$

Similar to the phase noise in a phase-locked loop, the noise is dominated by the reference source near the carrier and by the oscillator itself far from the carrier. It is noticeable from (9) and (10) that the noise bandwidth of an injection-locked oscillator is equal to the locking bandwidth that is determined by the injected power. We need to point out that this property reduces the design flexibility and is not desirable when narrow noise bandwidth is required.

A 4×4 and a 6×6 grid oscillator arrays were used in the injection locking experiment. The two arrays, which can pro-

TABLE I
Measured Phase Noise of the Loop-Phase-Locked Grid Oscillator Array and the Reference Source

Offset Frequency	100Hz	1kHz	10kHz	100kHz	1MHz
Locked Grid	73dBc	78dBc	84dBc	88dBc	106dBc
Synthesizer*	70dBc	78dBc	86dBc	107dBc	N/A

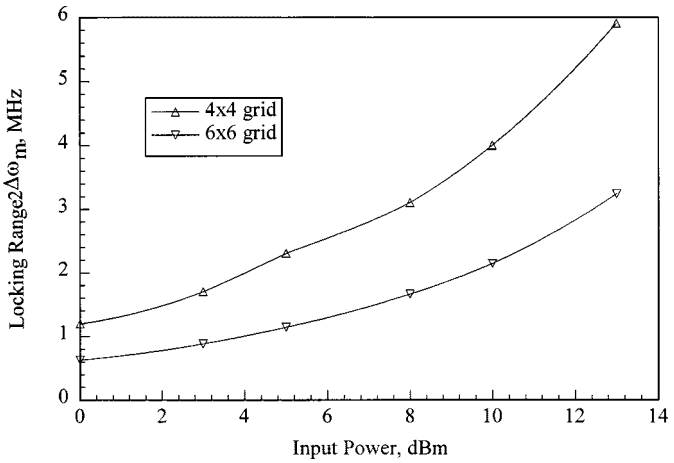

Fig. 12. Locking range of injection-locked 4 × 4 and 6 × 6 grid oscillators.

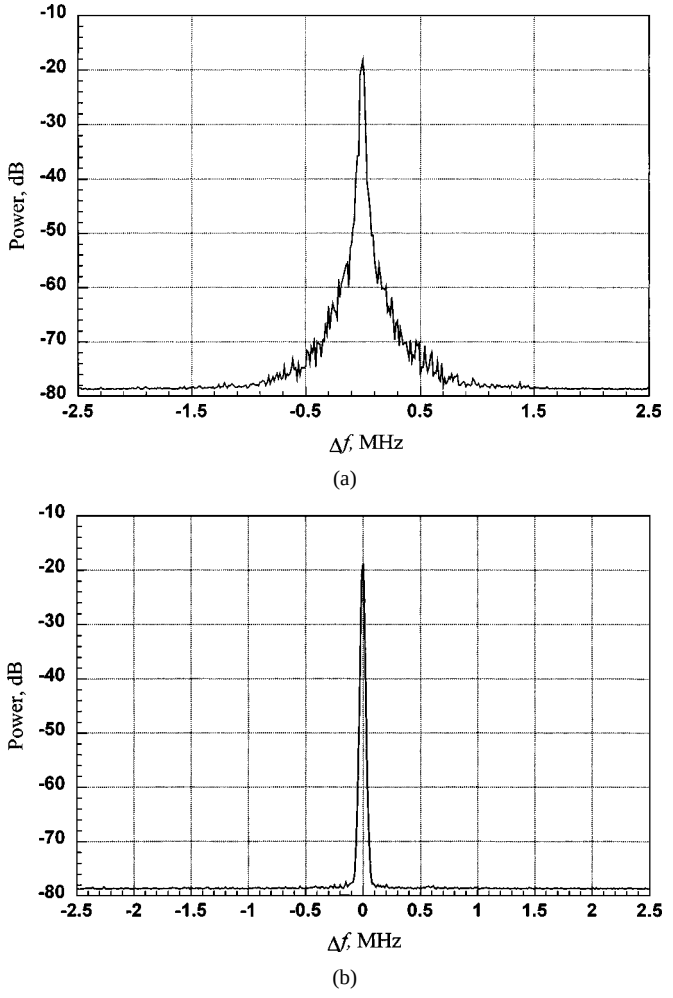

Fig. 13. Spectra of: (a) free-running and (b) injection-locked 6 × 6 grid oscillator array. Center frequency: 4.2 GHz. Spectrum analyzer filter bandwidth: 3 kHz.

duce 31 and 35 dBm at approximately 5.1 and 4.4 GHz, respectively, are described in [15]. In order to couple the injection signal to the grid arrays, the same loop antenna structure as shown in Fig. 8 was used for injecting the reference signal. The injected signal power was radiated by the loop antenna and coupled to the nearby unit cells in the grid oscillator array. Injection locking takes place when the injected signal frequency

TABLE II
MEASURED PHASE NOISE OF THE INJECTION-LOCKED 4 × 4 GRID OSCILLATOR ARRAY

Offset Frequency	100Hz	1kHz	10kHz	100kHz	1MHz
Pin=0 dBm	65dBc	70dBc	75dBc	85dBc	105dBc
Pin=3 dBm	65dBc	70dBc	80dBc	90dBc	105dBc
Pin=5 dBm	70dBc	75dBc	83dBc	95dBc	105dBc
Pin=8 dBm	70dBc	75dBc	80dBc	90dBc	110dBc
Pin=10 dBm	73dBc	80dBc	85dBc	95dBc	110dBc
Pin=13 dBm	75dBc	80dBc	85dBc	105dBc	115dBc

TABLE III
MEASURED PHASE NOISE OF THE INJECTION-LOCKED 6 × 6 GRID OSCILLATOR ARRAY

Offset Frequency	100Hz	1kHz	10kHz	100kHz	1MHz
Pin=0 dBm	60dBc	70dBc	75dBc	90dBc	110dBc
Pin=3 dBm	65dBc	75dBc	80dBc	90dBc	110dBc
Pin=5 dBm	65dBc	75dBc	80dBc	95dBc	110dBc
Pin=8 dBm	70dBc	80dBc	85dBc	100dBc	115dBc
Pin=10 dBm	70dBc	80dBc	85dBc	100dBc	115dBc
Pin=13 dBm	70dBc	85dBc	85dBc	105dBc	115dBc

is close to the grid oscillator frequency. Fig. 12 shows the measured locking ranges for both 4 × 4 and 6 × 6 grid oscillator arrays as functions of the injected power. Notice that this power is not the same power as it is in (8). The narrow locking range is due to a poor matching of the loop antenna. Our measurement using an HP8719C network analyzer showed that the measured return loss of the loop antenna was only −0.3 dB at 4.5 GHz, which means that only 7% of the power was radiated into the grid array. Wider locking range can be obtained by improving the impedance matching of the loop antenna. We can also observe from the figure that the locking range for the 6 × 6 array is approximately half of the locking range for the 4 × 4 array. This is not surprising since the power coupled to the unit cells nearby the loop antenna is the same for both arrays, while the Q factor of the 6 × 6 array is approximately two times as that of the 4 × 4 grid oscillator array [10].

Fig. 13 shows the spectra of the free-running 6 × 6 grid oscillator and the injection-locked 6 × 6 grid oscillator. It can be seen from this figure that the spectrum linewidth narrows significantly when the grid oscillator is injection locked to a microwave frequency synthesizer.

Tables II and III list the phase noise performances, measured in the same way as we did for the loop-phase-locked grid oscillator array, of the injection-locked 4 × 4 and 6 × 6 grid oscillator

arrays, respectively. Although this data is just a rough measurement due to the instrument limitations, one can still notice that the injection-locked 6×6 grid oscillator array has lower phase noise at high frequency-off-carrier. This manifests the fact that the Q factor in a larger coupled oscillator arrays is higher than that in a smaller coupled oscillator arrays and, hence, a larger coupled oscillator array has better phase noise performance.

V. Conclusion

Work has successfully been done on the frequency stabilization of power-combining grid oscillator arrays by means of both the loop-phase-locking and injection-locking techniques. It also demonstrated that the phase locking of a quasi-optical oscillator does not necessarily require that the taking of a sampling signal or injection of a reference signal must be taken quasi-optically. The use of simple devices like loop antenna or slot antenna on the reflector mirror can greatly reduce the complexity of the quasi-optical system.

In comparison, injection locking of a grid oscillator array is straightforward, and does not require that the grid oscillator array be electrically tunable, as it does in a phase-locked loop. The noise bandwidth can be adjusted simply by changing the injected signal power. The changing of injected power, however, also affects the locking range, which is a undesirable feature. The loop-phase-locking technique can provide flexibility in the design since the locking range and noise bandwidth can be designed separately. It also has better oscillator phase noise rejection when a second-order loop is used (first-order frequency response for injection locking).

Acknowledgment

The authors would like to express their appreciation to Dr. J. E. Harriss, Clemson University, Clemson, SC, for assistance in fabrication of the 16-element array, Dr. G. Guo, TRW, Redondo Beach, CA, for his initial contributions to this effort. The authors also extend thanks to Dr. G. David, The University of Michigan at Ann Arbor, K. Yang, The University of Michigan at Ann Arbor, Dr. L. B. Katehi, The University of Michigan at Ann Arbor, and Dr. J. Whitaker, The University of Michigan at Ann Arbor, for their help on measuring the spectra with their spectrum analyzer and LabView during a time when the field distribution of this oscillator was being characterized in their electrooptic imaging system.

References

[1] J. W. Mink, "Quasi-optical power combining of solid-state millimeter wave sources," *IEEE Trans. Microwave Theory Tech.*, vol. MTT-34, pp. 273–279, Feb. 1986.
[2] J. C. Wiltse and J. W. Mink, "Quasioptical power combining of solid state sources," *Microwave J.*, vol. 35, no. 2, pp. 144–156, Feb. 1992.
[3] E. R. Brown and J. F. Harvey, "Research focus on quasioptical technology," *Microwave J.*, vol. 41, no. 9, pp. 22–35, Sept. 1998.
[4] J. A. Navarro and K. Chang, *Integrated Active Antennas and Spatial Power Combining*. New York: Wiley, 1996, p. 368.
[5] R. A. York and Z. B. Popović, *Active and Quasi-Optical Arrays for Solid-State Power Combining*, ser. Microwave Opt. Eng. New York: Wiley, 1997.
[6] N. S. Chang, T. P. Dao, M. G. Case, D. B. Rensch, and R. A. York, "60 W X-band spatially combined solid state amplifier," in *IEEE MTT-S Int. Microwave Symp. Dig.*, 1999, pp. 539–542.
[7] J. B. Hacker, M. P. De Lisio, M. Kim, C.-M. Liu, S.-J. Li, S. W. Wedge, and D. B. Rutledge, "A 10-watt X-band grid oscillator," in *IEEE MTT-S Int. Microwave Symp. Dig.*, San Diego, CA, June 1994, pp. 823–826.
[8] W. A. Shiroma, B. L. Shaw, and Z. B. Popović, "Three-dimensional power combiners," in *IEEE MTT-S Int. Microwave Symp. Dig.*, San Diego, CA, June 1994, pp. 831–834.
[9] R. J. Dinger, D. J. White, and D. Bowling, "A 10 GHz space power combiner with parasitic injection locking," in *IEEE MTT-S Int. Microwave Symp. Dig.*, Baltimore, MD, June 1986, pp. 163–165.
[10] H.-C. Chang, X. Cao, M. J. Vaughan, U. K. Mishra, and R. A. York, "Phase noise in externally injection-locked oscillator arrays," *IEEE Trans. Microwave Theory Tech.*, vol. 45, pp. 2035–2042, Nov. 1997.
[11] T. Mader, S. Bundy, and Z. B. Popović, "Quasi-optical VCOs," *IEEE Trans. Microwave Theory Tech.*, vol. 39, no. 41, pp. 1725–1781, Oct. 1993.
[12] A. C. Oak and R. M. Weikle, II, "A varactor-tuned 16-element MESFET grid oscillator," in *IEEE Int. AP-S Int. Symp.*, Newport Beach, CA, June 1995, pp. 1296–1264.
[13] L. Q. Sun and R. M. Weikle, II, "Varactor-controlled HFET oscillator grids," in *IEEE Int. AP-S Int. Symp.*, Montreal, QC, Canada, July 1997, pp. 2460–2463.
[14] W. Wang and L. W. Pearson, "Attaining wide tuning range in quasioptical voltage controlled grid oscillators," in *Proc. 26th Eur. Microwave Conf.*, Prague, Czech Republic, Sept. 1996, pp. 681–684.
[15] ——, "Experimental study of finite planar grid oscillator arrays," *Int. J. Infrared Millim. Waves*, vol. 22, no. 7, pp. 1287–1305, July 1999.
[16] M. Gouker, "Toward standard figures-of-merit for spatial and quasi-optical power combining arrays," *IEEE Trans. Microwave Theory Tech.*, vol. 43, pp. 1614–1616, July 1995.
[17] V. Manassewitsch, *Frequency Synthesizers, Theory and Design*. New York: Wiley, 1987.
[18] B. Roth and A. Beyer, "Measurement techniques for microwave oscillators," presented at the IEEE MTT-S Int. Microwave Symp. Workshop, Orlando, FL, May 1995.
[19] K. Kurokawa, "Injection locking of microwave solid-state oscillators," *Proc. IEEE*, vol. 61, pp. 1386–1410, Oct. 1973.
[20] M. E. Hines, J. C. R. Collinet, and J. G. Ondria, "FM noise suppression of an injection phase-locked oscillator," *IEEE Trans. Microwave Theory Tech.*, vol. MTT-16, pp. 738–742, Sept. 1968.

Wenzhang Wang (S'95–M'98) received the B.Sc. and M.Sc. degrees in radio engineering from Southeast University, Nanjing, China, in 1984 and 1987, respectively, and the Ph.D. degree in electrical engineering from Clemson University, Clemson, SC, in 1998.

From 1987 to 1992, he was a Research Engineer with the National Institute of Metrology, Beijing, China, where he designed highly stable phase-locked millimeter-wave sources for China's national frequency and voltage standard applications and laser frequency measurement systems. From 1993 to 1998, he was a Research Assistant with Clemson University, where he was involved with research on quasi-optical power-combining techniques. Since 1998, he has been with the Telaxis Communications Corporation (formerly Millitech Corporation), South Deerfield, MA, where he designed various kinds of millimeter-wave transmitters and receivers. His research interests include numerical modeling of electromagnetic (EM) structures, spatial power-combining techniques, integrated millimeter-wave circuits and systems, and their applications in local multipoint distribution system (LMDS) and point-to-point radios.

L. Wilson Pearson (S'64–M'69–F'91) received the B.S. and M.S. degrees from the University of Mississippi, University, and the Ph.D. degree from The University of Illinois at Urbana-Champaign, all in electrical engineering.

He has served on the faculties of the University of Kentucky, University of Mississippi, as an Affiliate Professor at Washington University, and as Senior Scientist and then Principal Scientist in Electromagnetic Signatures at the McDonnell Douglas Research Laboratories, St. Louis, MO. He was also with the Naval Surface Weapons Center. He was the Head of the Department of Electrical and Computer Engineering Department, Clemson University. He is currently the Director of the Center for Research in Wireless Communications, Clemson University. He also currently leads a multiuniversity team of workers (The University of Leeds, The University of Michigan at Ann Arbor, University of Illinois, and North Carolina State University) in a Multidisciplinary University Research Initiative (MURI) on spatial power combining at millimeter wavelengths. His research interests include experimental and computational methods in electrical and RF systems. His application areas include communications, electromagnetic scattering, and RF imaging in battlefield and automotive applications.

Dr. Pearson is a member of Commissions B and D of the U.S. National Committee of the International Union for Radio Science (URSI). He has served on the Administrative Committee (AdCom) for the IEEE Antennas and Propagation Society (IEEE AP-S), as secretary of the Electromagnetics Society, and as the Technical Program Committee chair for the 1998 International Symposium on Antennas and Propagation/URSI National Radio Science Meeting. He was editor-in-chief for the IEEE TRANSACTIONS ON ANTENNAS AND PROPAGATION and is currently on the Editorial Board of the PROCEEDINGS OF THE IEEE. He is the vice president of the IEEE AP-S. He was a recipient of an IEEE Third Millennium Medal.